

CTP-TAMU-45/96
 DOE/ER/40717-33
 ACT-13/96
 hep-ph/9609524

Supersymmetric Photonic Signals at LEP

Jorge L. Lopez¹, D.V. Nanopoulos^{2,3}, and A. Zichichi⁴

¹Department of Physics, Bonner Nuclear Lab, Rice University
 6100 Main Street, Houston, TX 77005, USA

²Center for Theoretical Physics, Department of Physics, Texas A&M University
 College Station, TX 77843-4242, USA

³Astroparticle Physics Group, Houston Advanced Research Center (HARC)
 The Mitchell Campus, The Woodlands, TX 77381, USA

⁴University and INFN-Bologna, Italy and CERN, 1211 Geneva 23, Switzerland

Abstract

We explore and contrast the single-photon and diphoton signals expected at LEP 2, that arise from neutralino-gravitino ($e^+e^- \rightarrow \chi\tilde{G} \rightarrow \gamma + E_{\text{miss}}$) and neutralino-neutralino ($e^+e^- \rightarrow \chi\chi \rightarrow \gamma\gamma + E_{\text{miss}}$) production in supersymmetric models with a light gravitino. LEP 1 limits imply that one may observe either one, but not both, of these signals at LEP 2, depending on the values of the neutralino and gravitino masses: single-photons for $m_\chi \gtrsim M_Z$ and $m_{\tilde{G}} \lesssim 3 \times 10^{-5}$ eV; diphotons for $m_\chi \lesssim M_Z$ and all allowed values of $m_{\tilde{G}}$.

September 1996

Searches for supersymmetry at colliders take on a new look in the case of models with a very light gravitino, where the lightest neutralino ($\chi_1^0 \equiv \chi$) is no longer the lightest supersymmetric particle and instead decays dominantly (in many models) into a photon and the gravitino (*i.e.*, $\chi \rightarrow \gamma \tilde{G}$) [1]. The γ – $\tilde{\gamma}$ – \tilde{G} effective interaction is inversely proportional to the gravitino mass [2] and yields an observable inside-the-detector decay for $m_{\tilde{G}} < 10^3$ eV [3]. On the other hand, the gravitino mass cannot be too small [4], as otherwise all supersymmetric particles would be strongly produced: $m_{\tilde{G}} > 10^{-6}$ eV appears required [4, 5]. Light gravitino scenarios were considered early on [2, 1], but have recently received considerable more attention because of their natural ability to explain the puzzling CDF $ee\gamma\gamma + E_{T,\text{miss}}$ event [6] via selectron or chargino pair-production [7, 3, 8]. Such scenarios have distinct experimental signatures, that always include one or more photons, which may be readily detected at LEP [9, 3, 8].

In the light gravitino scenario, the most accessible supersymmetric processes at LEP are $e^+e^- \rightarrow \chi\tilde{G} \rightarrow \gamma + E_{\text{miss}}$ and $e^+e^- \rightarrow \chi\chi \rightarrow \gamma\gamma + E_{\text{miss}}$. The single-photon and diphoton processes differ in their dependence on the gravitino mass: the rate for the first process is proportional to $m_{\tilde{G}}^{-2}$, whereas the second is independent of the gravitino mass. These processes also differ in their kinematical reach: $m_\chi < \sqrt{s}$ versus $m_\chi < \frac{1}{2}\sqrt{s}$. However, one must also consider their threshold behavior, which for the single-photon process goes as β^8 [4] whereas for the diphoton process goes as β^3 [10], thus compensating somewhat the different kinematical reaches.

In this note we explore and contrast the single-photon and diphoton signals at LEP 2. The diphoton process has been considered in detail previously [9, 3, 8]. The single-photon process was originally considered by Fayet [4] in the restricted case of a very light photino-like neutralino. This process was revisited in the context of LEP 1, although only in the restricted case of a non-negligible zino component of the neutralino, where the resonant Z -exchange diagram dominates [11]. We have recently generalized the single-photon calculation to arbitrary center-of-mass energies and neutralino compositions, details of which appear elsewhere [12].

Let us start by considering the limits that LEP 1 imposes on the single-photon process. At $\sqrt{s} = M_Z$, this process proceeds dominantly through s -channel Z exchange via the coupling Z – \tilde{Z} – \tilde{G} , which is proportional to the zino component of the neutralino N'_{12} .¹ The non-resonant contributions, s -channel photon exchange and t -channel $\tilde{e}_{R,L}$ exchange, are negligible unless the zino component of the neutralino is small ($N'_{12} < 0.2$), in which case one must include all (resonant and non-resonant) diagrams in the calculation. The explicit expression for the cross section in the general case is given in Ref. [12]. Here we limit ourselves to note its dependence on $m_{\tilde{G}}$ and its threshold behavior, which is valid for all values of \sqrt{s} and all neutralino

¹In the notation of Ref. [13], the lightest neutralino can be written as $\chi \equiv \chi_1^0 = N'_{11}\tilde{\gamma} + N'_{12}\tilde{Z} + N_{13}\tilde{H}_1^0 + N_{14}\tilde{H}_2^0$ or alternatively as $\chi_1^0 = N_{11}\tilde{B} + N_{12}\tilde{W}_3 + N_{13}\tilde{H}_1^0 + N_{14}\tilde{H}_2^0$, where $N'_{11} = N_{11} \cos \theta_W + N_{12} \sin \theta_W$ and $N'_{12} = -N_{11} \sin \theta_W + N_{12} \cos \theta_W$.

compositions:

$$\sigma(e^+e^- \rightarrow \chi\tilde{G}) \propto \frac{1}{m_{\tilde{G}}^2} \left(1 - \frac{m_\chi^2}{s}\right)^4. \quad (1)$$

This β^8 threshold behavior results from subtle cancellations among all contributing amplitudes and was first pointed out by Fayet [4] in the case of pure-photino neutralinos. Dimensional analysis indicates that this cross section is of electroweak strength (or stronger) when $M_Z^4/(M_{\text{Pl}}^2 m_{\tilde{G}}^2) \sim 1$ or $m_{\tilde{G}} \sim M_Z^2/M_{\text{Pl}} \sim 10^{-5} \text{ eV}$ (or smaller).

A numerical evaluation of the single-photon cross section versus the neutralino mass for $m_{\tilde{G}} = 10^{-5} \text{ eV}$ is shown in Fig. 1, for different choices of neutralino composition ('zino': $N'_{12} = 1$; 'bino': $N_{11} = 1$, and 'photino': $N'_{11} = 1$), and where we have assumed the typical result $B(\chi \rightarrow \gamma\tilde{G}) = 1$. In the photino case the Z -exchange amplitude is absent ($N'_{11} = 1 \Rightarrow N'_{12} = 0$) and one must also specify the selectron masses which mediate the t -channel diagrams: we have taken the representative values $m_{\tilde{e}_R} = m_{\tilde{e}_L} = 75, 150 \text{ GeV}$.

In Fig. 1 we also show (dotted line 'LNZ') the results for a well-motivated one-parameter no-scale supergravity model [8, 14], which realizes the light gravitino scenario that we study here. In this model the neutralino is mostly gaugino, but has a small higgsino component at low values of m_χ , which disappears with increasing neutralino masses; the neutralino approaches a pure bino at high neutralino masses. The selectron masses also vary (increase) continuously with the neutralino mass and are not degenerate (*i.e.*, $m_{\tilde{e}_L} \sim 1.5 m_{\tilde{e}_R} \sim 2m_\chi$).

Our particular choice of $m_{\tilde{G}} = 10^{-5} \text{ eV}$ in Fig. 1 leads to observable single-photon cross sections above the Z peak; otherwise the curves scale with $1/m_{\tilde{G}}^2$. The dashed line indicates our estimate of the LEP 1 upper limit on the single-photon cross section of 0.1 pb [15]. This estimate is an amalgamation of individual experiment limits with partial LEP 1 luminosities ($\sim 100 \text{ pb}^{-1}$) and angular acceptance restrictions ($|\cos \theta_\gamma| < 0.7$). Note that the single-photon background at the Z peak (mostly from $e^+e^- \nu\bar{\nu}\gamma$) is quite significant, as otherwise one would naively expect upper bounds of order $3/\mathcal{L} < 0.03 \text{ pb}$. Imposing our estimated LEP 1 upper limit one can obtain a lower bound on the gravitino mass as a function of the neutralino mass, which in some regions of parameter space is as strong as $m_{\tilde{G}} > 10^{-3} \text{ eV}$, but of course disappears for $m_\chi > M_Z$ (see Ref. [12] for details).

As of this writing there are no reported excesses in the single-photon cross sections measured at $\sqrt{s} = 130, 133, 140, 161 \text{ GeV}$. However, as it is not clear what the actual experimental sensitivity to these processes is, we refrain from imposing further constraints from LEP 1.5 and LEP 2 searches. To stimulate the experimental study of this process, in Fig. 2 we show the single-photon cross sections calculated at $\sqrt{s} = 161 \text{ GeV}$. (Further elaborations, including cross sections at other energies and photonic energy and angular distributions appear in Ref. [12].) Note that the cross sections increase with increasing selectron masses (saturating at values somewhat larger than the ones shown), and conversely decrease with decreasing selectron masses. This behavior is expected: in the limit of unbroken supersymmetry (*i.e.*, for massless selectrons and photinos) the gravitino loses its longitudinal spin- $\frac{1}{2}$ component, and

therefore amplitudes involving it must vanish. This is the case in our calculations, as only the spin- $\frac{1}{2}$ ‘goldstino’ component of the gravitino becomes enhanced for light gravitino masses. Alternatively, the effective e – \tilde{e} – \tilde{G} coupling is proportional to $m_{\tilde{e}}^2$ and the t -channel amplitude goes as $m_{\tilde{e}}^2/(t - m_{\tilde{e}}^2)$, showing the dependence on $m_{\tilde{e}}$ and its saturation for large values of $m_{\tilde{e}}$; at threshold $t \rightarrow 0$ and the t -channel amplitude becomes independent of $m_{\tilde{e}}$ and combines with the other amplitudes to yield the β^8 threshold behavior [12].

Note also that the photino, bino, and zino cross sections become comparable above the Z pole, when the Z -exchange diagram becomes comparable to the other diagrams. In the case of the one-parameter model (‘LNZ’) a peculiar bump appears. This bump is understood in terms of the selectron masses that vary continuously with the neutralino mass: at low values of m_χ the selectron masses are light and the cross section approaches the light fixed-selectron mass curves (‘75’); at larger values of m_χ the selectron masses are large and the cross section approaches (and exceeds) the heavy fixed-selectron mass curves (‘150’). This example brings to light some of the subtle features that might arise in realistic models of low-energy supersymmetry.

We now turn to the diphoton signal, which proceeds via s -channel Z -exchange and t -channel selectron ($\tilde{e}_{R,L}$) exchange, and does not depend on $m_{\tilde{G}}$. The Z -exchange contribution is present only when the neutralino has a higgsino component (*c.f.* the single-photon signal where the reverse is true), whereas the t -channel contribution is present only when the neutralino has a gaugino component (the higgsino component couples to the electron mass). The numerical results for the diphoton cross section at $\sqrt{s} = 161$ GeV for various neutralino compositions are shown in Fig. 3,² and exhibit the expected β^3 behavior [10]. We should first comment on the corresponding results at the Z -peak [12], which exhibit a great enhancement when the neutralino has a non-negligible higgsino component (as is the case in the ‘LNZ’ model). It is not clear what is the LEP 1 limit on the diphoton cross section, especially in the presence of substantial E_{miss} . If the LEP 1 diphoton limit is comparable to the single-photon one, the corresponding ‘LNZ’ and ‘higgsino’ curves would be excluded up to the kinematical limit (*i.e.*, $m_\chi > \frac{1}{2}M_Z$), but in models with purely gaugino neutralinos all limits could be evaded by increasing the selectron mass sufficiently [12].

Moving on to higher LEP energies, limits on acoplanar photon pairs at LEP 1.5 have been released by OPAL [16] and DELPHI [17], and they amount to upper bounds of 2.0 pb and 1.5 pb respectively. Imposing these limits on the ‘LNZ’ model as an example entails $m_\chi > 37$ GeV [8]. Coming back to LEP161, diphoton limits are available from DELPHI ($\sigma < 3.1$ pb with $\mathcal{L} = 2.8 \text{ pb}^{-1}$ [17]) and ALEPH ($\sigma < 1.0$ pb with $\mathcal{L} = 4.4 \text{ pb}^{-1}$ [18]). These limits are expected to improve somewhat once the full LEP161 dataset is analyzed. Nonetheless, Fig. 3 shows that the present ALEPH limit imposes new constraints beyond those possible at LEP 1 or LEP 1.5 (*e.g.*, in the ‘LNZ’ model $m_\chi > 46$ GeV is required).

Comparing Fig. 2 with Fig. 3, it is amusing to note that the dependence on the

²In Fig. 3 the ‘higgsino’ curve corresponds to the choice $N_{13} = 1$, which maximizes the higgsino contribution. Otherwise the cross section scales as $[(N_{13})^2 - (N_{14})^2]^2$.

selectron masses is reversed from one case to the other: the single-photon (diphoton) rate increases (decreases) with increasing selectron masses. The former behavior was explained above, the latter behavior is the usual one. The dependence on the neutralino composition is also reversed from one case to the other: zino's dominate the single-photon rate because of their Z -pole enhancement, bino's have some zino component and come close, while photinos have no zino component and come in last. The diphoton rate for gaugino-like neutralinos proceeds only via t -channel selectron exchange and depends crucially on the coupling of left- and right-handed selectrons to neutralinos: (in units of e)

$$\begin{array}{ccc}
 \tilde{e}_R & \tilde{e}_L & \\
 \tilde{\gamma} & 1 & 1 \\
 \tilde{B} & \frac{1}{\cos \theta_W} & \frac{1}{2 \cos \theta_W} \\
 \tilde{Z} & \frac{\sin \theta_W}{\cos \theta_W} & \frac{-\frac{1}{2} + \sin^2 \theta_W}{\sin \theta_W \cos \theta_W}
 \end{array} = \begin{array}{ccc}
 \tilde{e}_R & \tilde{e}_L & \\
 \tilde{\gamma} & 1.00 & 1.00 \\
 \tilde{B} & 1.14 & 0.57 \\
 \tilde{Z} & 0.55 & 0.64
 \end{array}$$

Note that in the bino case the coupling to left- and right-handed selectrons differs by a factor of 2, which becomes a factor of 16 in the contributions to the cross section. For equal mass selectrons, the relative sizes of the photino, bino, and zino results in Fig. 3 follow easily from these couplings.

The striking point of this paper is obtained by comparing the single-photon versus diphoton cross sections at, for example, $\sqrt{s} = 190$ GeV, once the LEP 1 limit on the single-photon cross section is imposed. To exemplify the result we take as a representative example the one-parameter ('LNZ') model [8], and plot both cross sections in Fig. 4, for two values of the gravitino mass. For $m_{\tilde{G}} = 10^{-5}$ eV (top panel), in principle both the single-photon (σ_{γ}^{190}) and diphoton ($\sigma_{\gamma\gamma}^{190}$) processes may be observable at LEP 2. However, the LEP 1 limit on the single-photon rate ($\sigma_{\gamma}^{M_Z}$) can only be satisfied for $m_{\chi} > 85$ GeV, and in this region the diphoton process becomes negligible. Thus in this case one may observe only single photons. Increasing the gravitino mass to ameliorate the LEP 1 constraint on $\sigma_{\gamma}^{M_Z}$ (to $m_{\tilde{G}} = 5 \times 10^{-4}$ eV, bottom panel), suppresses the single-photon rate at LEP 1 by a factor of $(50)^2$, but it suppresses the single-photon rate at LEP190 by the same factor, rendering it unobservable. However, the diphoton process at LEP190 now becomes allowed for any value of the neutralino mass (consistent with LEP 1 and LEP 1.5 limits), and this time one may observe only diphotons. Neither intermediate values of the gravitino mass nor lower center-of-mass energies change this picture. Requiring a minimum observable single-photon cross section of 0.1 pb, we obtain two mutually exclusive scenarios: single-photons for $m_{\chi} \gtrsim M_Z$ and $m_{\tilde{G}} \lesssim 3 \times 10^{-5}$ eV; diphotons for $m_{\chi} \lesssim M_Z$ and all allowed values of $m_{\tilde{G}}$.

We have verified that the same general result holds for the various other neutralino compositions that we have explored above, although in some small regions of parameter space there is a small overlap region where both single-photon and diphoton signals may be simultaneously observable. However, this may only occur for the highest LEP energies and smallest gravitino masses ($m_{\tilde{G}} \sim 10^{-5}$ eV), and only very near the diphoton kinematical limit, where the diphoton cross section is small.

In sum, we have explored the photonic signals that may be observed at LEP in models with a light gravitino, where single-photon and diphoton signals play a complementary role, and have the advantage over any other supersymmetric signal of the largest reach into parameter space. This study is intended to stimulate our experimental colleagues to undertake the experimental work required to extract the limits and sensitivities to the single-photon and diphoton signals at above-the- Z -peak energies.

The work of J. L. has been supported in part by DOE grant DE-FG05-93-ER-40717. The work of D.V.N. has been supported in part by DOE grant DE-FG05-91-ER-40633.

References

- [1] J. Ellis, K. Enqvist, and D. Nanopoulos, Phys. Lett. B **147** (1984) 99. See also, J. Ellis, K. Enqvist, and D. Nanopoulos, Phys. Lett. B **151** (1985) 357.
- [2] P. Fayet, Phys. Lett. B 69 (1977) 489; B 70 (1977) 461; B 84 (1979) 421; B 86 (1979) 272.
- [3] S. Ambrosanio, G. Kane, G. Kribs, S. Martin, and S. Mrenna, Phys. Rev. Lett. **76** (1996) 3498 and hep-ph/9605398.
- [4] P. Fayet, Phys. Lett. B **175** (1986) 471.
- [5] D. Dicus, S. Nandi, and J. Woodside, Phys. Rev. D **41** (1990) 2347, Phys. Rev. D **43** (1991) 2951.
- [6] S. Park, in Proceedings of the 10th Topical Workshop on Proton-Antiproton Collider Physics, Fermilab, 1995, edited by R. Raja and J. Yoh (AIP, New York, 1995), p. 62.
- [7] S. Dimopoulos, M. Dine, S. Raby, and S. Thomas, Phys. Rev. Lett. **76** (1996) 3494; S. Dimopoulos, S. Thomas, and J. Wells, Phys. Rev. D **54** (1996) 3283; K. Babu, C. Kolda, and F. Wilczek, hep-ph/9605408.
- [8] J. L. Lopez and D. V. Nanopoulos, hep-ph/9607220 (Mod. Phys. Lett. A, to appear) and hep-ph/9608275.
- [9] D. Stump, M. Wiest, and C.-P. Yuan, Phys. Rev. D **54** (1996) 1936.
- [10] J. Ellis and J. Hagelin, Phys. Lett. B **122** (1983) 303.
- [11] D. Dicus, S. Nandi, and J. Woodside, Phys. Lett. B **258** (1991) 231.
- [12] J. L. Lopez, D. V. Nanopoulos, and A. Zichichi, in preparation.
- [13] H. Haber and G. Kane, Phys. Rep. **117** (1985) 75.
- [14] J. L. Lopez, D. V. Nanopoulos, and A. Zichichi, Phys. Rev. D **49** (1994) 343 and Int. J. Mod. Phys. A **10** (1995) 4241.
- [15] O. Adriani, *et. al.* (L3 Collaboration), Phys. Lett. B **297** (1992) 469; R. Akers, *et. al.* (OPAL Collaboration), Z. Phys. C **65** (1995) 47; P. Abreu, *et. al.* (DELPHI Collaboration), CERN-PPE/96-03.
- [16] G. Alexander, *et.al.* (OPAL Collaboration), Phys. Lett. B **377** (1996) 222.
- [17] F. Barao, *et.al.* (DELPHI Collaboration), DELPHI 96-125 CONF 49 (submitted to ICHEP'96).
- [18] J. Dann (ALEPH Collaboration), presented at DPF96 (August 1996).

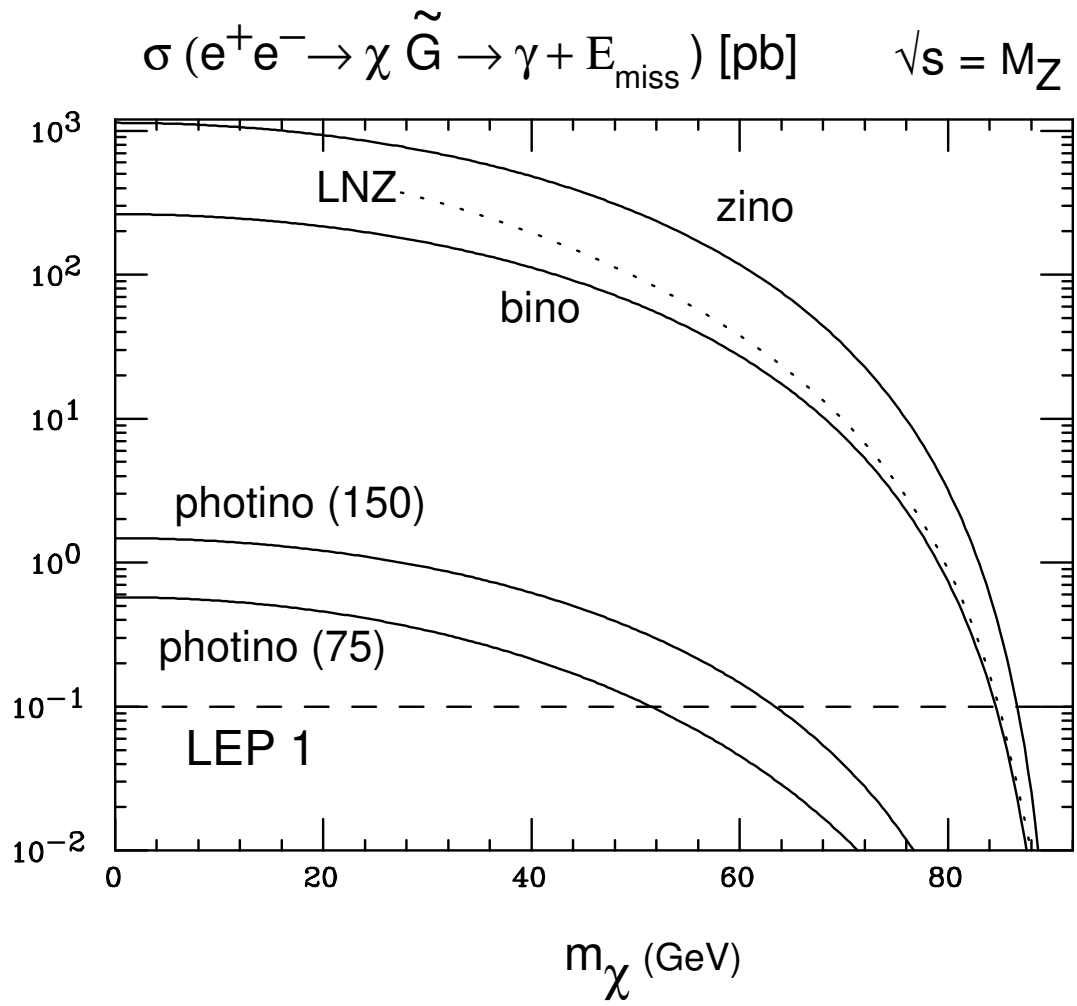


Figure 1: Single-photon cross sections (in pb) from neutralino-gravitino production at LEP 1 versus the neutralino mass (m_χ) for $m_{\tilde{G}} = 10^{-5} \text{ eV}$ and various neutralino compositions. The ‘photino’ curves depend on the selectron mass (75,150). The cross sections scale like $\sigma \propto m_{\tilde{G}}^{-2}$. The dashed line represents the estimated LEP 1 upper limit.

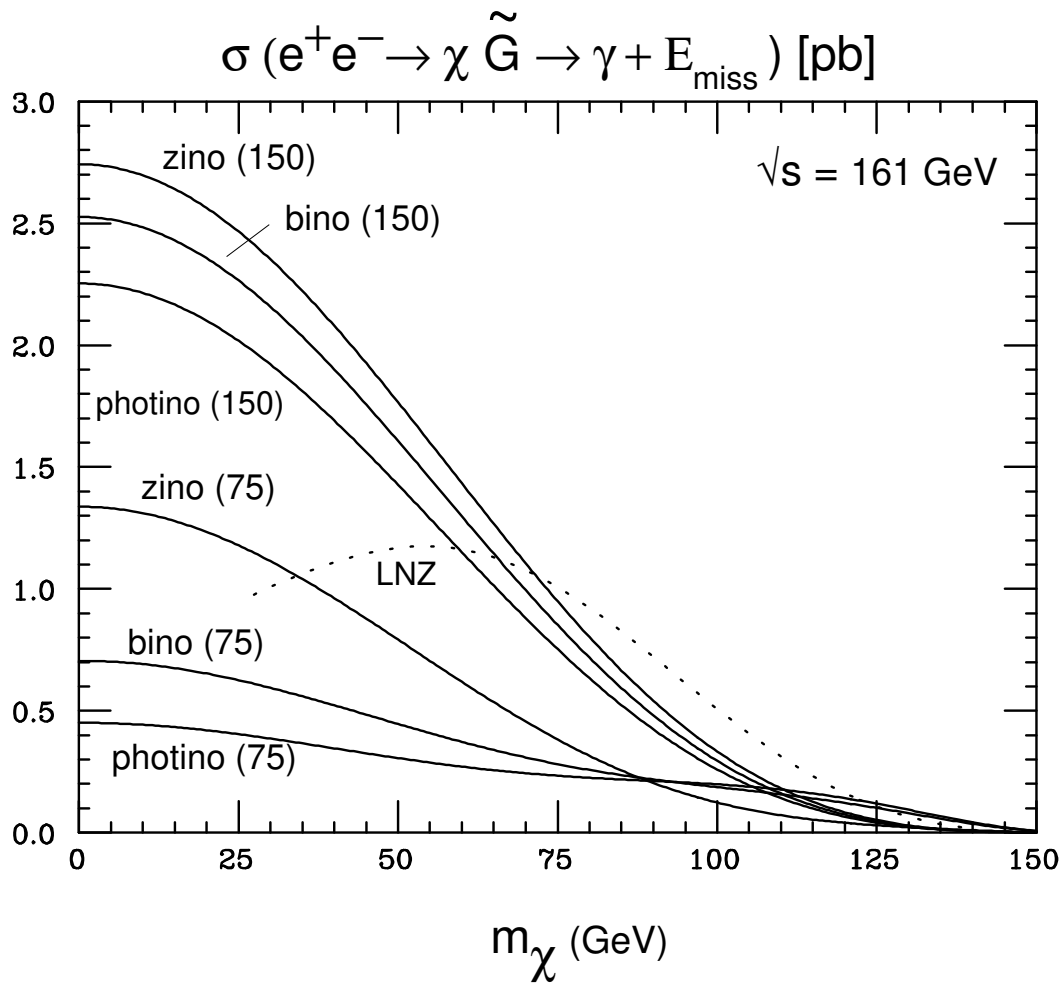


Figure 2: Single-photon cross sections (in pb) from neutralino-gravitino production at LEP 161 versus the neutralino mass (m_χ) for $m_{\tilde{G}} = 10^{-5} \text{ eV}$ and various neutralino compositions. The solid curves have a fixed value for the selectron mass (75,150), whereas the dotted curve corresponds to a one-parameter no-scale supergravity model where the selectron masses vary continuously with the neutralino mass. The cross sections scale like $\sigma \propto m_{\tilde{G}}^{-2}$.

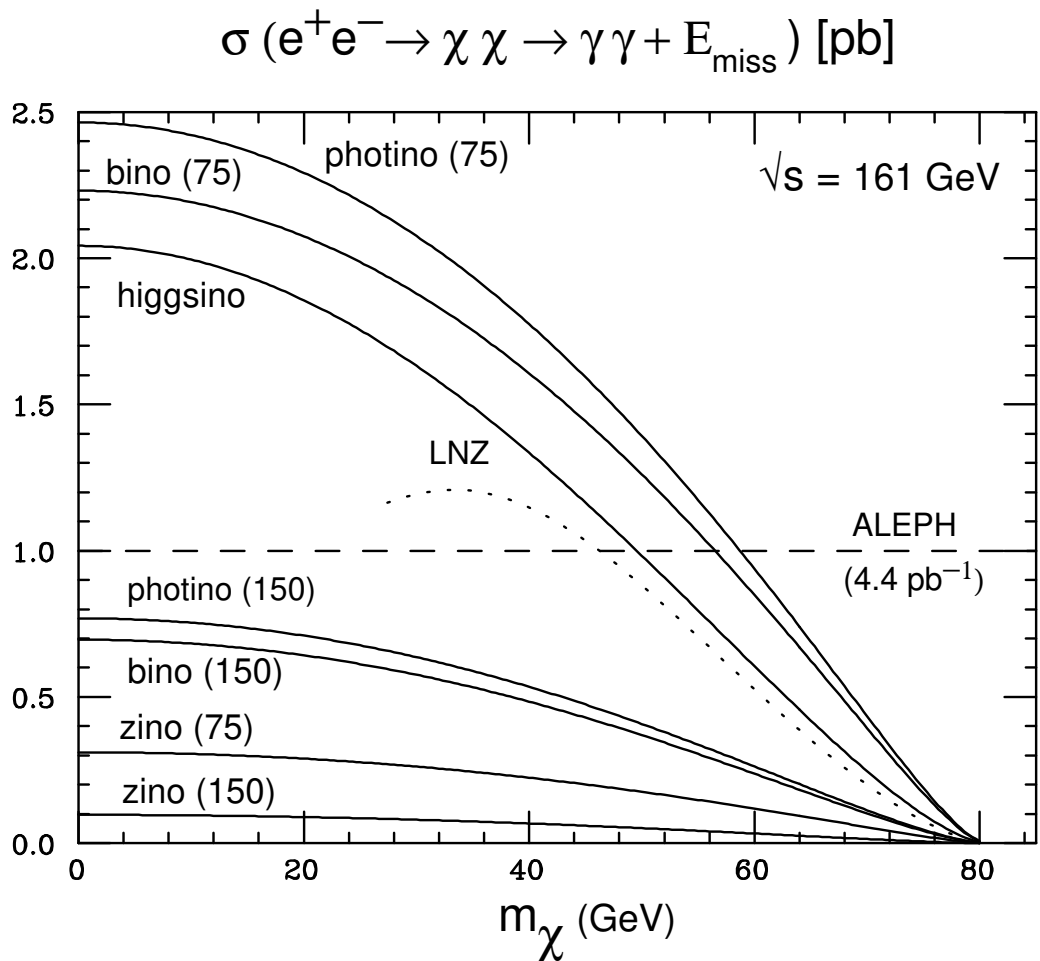


Figure 3: Diphoton cross sections (in pb) from neutralino-neutralino production at LEP161 versus the neutralino mass (m_χ) for various neutralino compositions. The dependence on the selectron mass is indicated (75,150) when relevant. The dashed line represents the preliminary ALEPH upper bound.

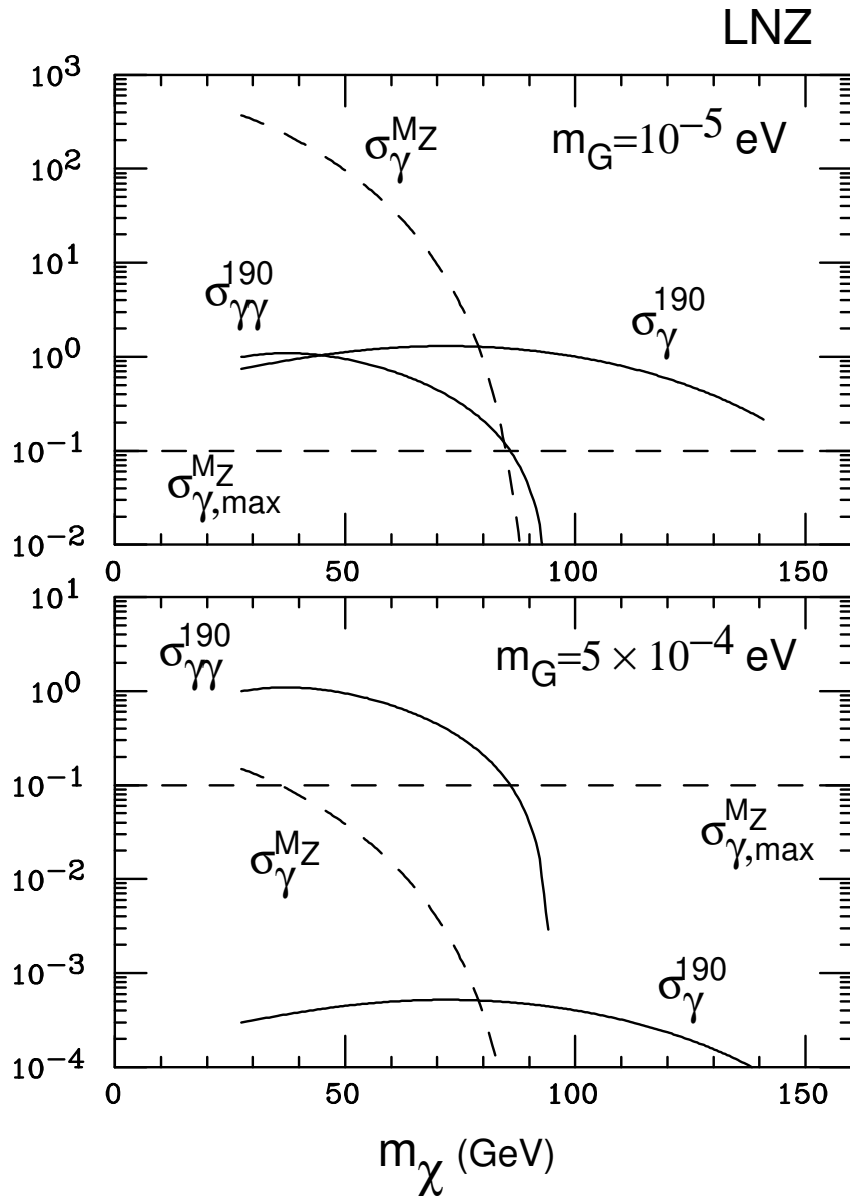


Figure 4: Comparison of single-photon (σ_γ^{190}) versus diphoton ($\sigma_{\gamma\gamma}^{190}$) signals (in pb) at LEP190 as a function of the neutralino mass, for two choices of the gravitino mass. The dashed lines represent the single-photon cross section ($\sigma_\gamma^{M_Z}$) and upper limit ($\sigma_{\gamma, \text{max}}$) at LEP 1. The one-parameter ‘LNZ’ model is taken here as a representative example of the two mutually exclusive scenarios that may be realized: either single photons or diphotos may be observed, but not both.